

Traffic of Molecular Motors

Stefan Klumpp, Melanie J. I. Müller and Reinhard Lipowsky

Max-Planck-Institut für Kolloid- und Grenzflächenforschung,
Wissenschaftspark Golm, 14424 Potsdam, Germany

Abstract. Molecular motors perform active movements along cytoskeletal filaments and drive the traffic of organelles and other cargo particles in cells. In contrast to the macroscopic traffic of cars, however, the traffic of molecular motors is characterized by a finite walking distance (or run length) after which a motor unbinds from the filament along which it moves. Unbound motors perform Brownian motion in the surrounding aqueous solution until they rebind to a filament. We use variants of driven lattice gas models to describe the interplay of their active movements, the unbound diffusion, and the binding/unbinding dynamics. If the motor concentration is large, motor-motor interactions become important and lead to a variety of cooperative traffic phenomena such as traffic jams on the filaments, boundary-induced phase transitions, and spontaneous symmetry breaking in systems with two species of motors. If the filament is surrounded by a large reservoir of motors, the jam length, i.e., the extension of the traffic jams is of the order of the walking distance. Much longer jams can be found in confined geometries such as tube-like compartments.

1 Introduction

The traffic of vesicles, organelles, protein complexes, messenger RNA, and even viruses within the cells of living beings is driven by the molecular motors of the cytoskeleton which move along cytoskeletal filaments in a directed fashion [1–3]. There are three large classes of cytoskeletal motors, kinesins and dyneins which move along microtubules, and myosins which move along actin filaments. These motors use the free energy released from the hydrolysis of adenosinetriphosphate (ATP), which represents their chemical fuel, for active movement and to perform mechanical work. They move in discrete steps in such a way that one molecule of ATP is used per step. Typical step sizes are ~ 10 nm, typical motor velocities are in the range of $\mu\text{m}/\text{sec}$.

Since the interior of cells is quite crowded and motors are strongly attracted by the filaments, which leads to relatively large motor densities along the filaments, it is interesting to study the collective traffic phenomena which arise from motor–motor interactions, in particular the formation of traffic jams due to the mutual exclusion of motors from filament sites. To study these cooperative phenomena theoretically we have introduced new variants of driven lattice gas models [4] which have been studied extensively during the last years both by our group [4–11] and by several other groups [12–17] and which will be described below. These models are related to lattice gas models for driven diffusive systems and exclusion processes as studied in the context of non-equilibrium phase

transitions [18–21] and highway traffic [22,23]. Since molecular motors can be studied in a systematic way using biomimetic systems which consist of a small number of components (such as motors, filaments, and ATP), they can also serve as model systems for the experimental investigation of driven diffusive systems.

Although the traffic of cargo particles pulled by molecular motors within cells is remarkably similar to the macroscopic traffic on streets or rails, there is an important difference which is a direct consequence of the nanoscale size of molecular motors: The motor–filament binding energy can be overcome by thermal fluctuations which are ubiquitous on this scale, and molecular motors therefore have a finite walking distance or run length after which they unbind from the filament along which they move. This walking distance is typically of the order of $1\ \mu\text{m}$ for a single motor molecule.¹ Likewise, unbound motors which diffuse freely in the surrounding aqueous solution, can bind to a filament and start active movement. In contrast to highway traffic, where additional cars enter only at on-ramps, i.e. at specific locations, binding of molecular motors occurs along the full length of the filaments. In addition to stepping along a one-dimensional track and mutual exclusion, lattice models for the traffic of molecular motors must therefore also describe the dynamics of motor–filament binding and unbinding as well as the diffusive movement of the unbound motors.²

In contrast to the transport properties of single motor molecules which have been studied extensively during the last 15 years [1,2], the traffic phenomena in many-motor systems have only recently attracted the interest of experimentalists and are still largely unexplored from the experimental point of view. The quantity of main interest has so far been the profile of the bound motor density along a filament. Density profiles with a traffic jam-like accumulation of motors at the end of filaments have been observed *in vivo* for a kinesin-like motor which was overexpressed in fungal hyphae [28,29]. Recently, motor traffic jams have also been observed in biomimetic *in vitro* systems using both conventional kinesin (kinesin 1) [30] and the monomeric kinesin KIF1A (kinesin 3) [17].

In the following, we will give a short overview over the lattice models for molecular motors and discuss the motor traffic in various systems which differ mainly in the compartment geometry and the arrangement of filaments. In section 4, we address the length of motor jams on filaments and argue that, in the presence of a large motor reservoir this jam length is typically of the order of the walking distance. Longer jams are found in confined geometries as discussed in section 5. In the last section of the paper, we briefly review our results for systems with two motor species.

¹ In order to transport a cargo actively over larger distances as, e.g., in the axon of a nerve cell, several motors work together in a cooperative fashion. We have recently shown that 7–8 motors are sufficient for processive transport over distances in the centimeter range as necessary in axons [24].

² These processes have not been taken into account in earlier studies of exclusion effects in many-motor systems which were based on ratchet models [25–27].

2 Lattice models for molecular motor traffic

To describe the interplay of the movements of bound and unbound motors, we have introduced a class of lattice models which incorporate the active movement of bound motors, the passive diffusion of unbound motors, and the motor–filament binding and unbinding dynamics [4]. These models can also account for motor–motor interactions such as their mutual exclusion from binding sites of the filament.

We describe the motor movements as random walks on a (in general, three-dimensional) cubic lattice as shown in Fig. 1(a). Certain lines on this lattice represent the filaments. The lattice constant is taken to be the motor step size ℓ which for many motors is equal to the filament periodicity. When a motor is localized at a filament site, it performs a biased random walk. Per unit time τ , it makes forward and backward steps with probabilities α and β , respectively. With probability γ , the motor makes no step and remains at the same site. The latter parameter is needed to account for the fact that if the lattice constant is given by the motor step size, unbound diffusion over this scale is much faster than an active step of a bound motor. Finally, the motor hops to each of the adjacent non-filament sites with probability $\epsilon/6$ and unbinds from the filament. The total unbinding probability per unit time is $\epsilon_0 = n_{\text{ad}}\epsilon/6$ with the number n_{ad} of adjacent non-filament sites which is given by $n_{\text{ad}} = 4$ and $n_{\text{ad}} = 3$ for filaments in solution and filaments immobilized to a surface, respectively.

At non-filament sites, the motor performs a symmetric random walk and hops to all neighboring sites with probability $1/6$ per time τ . This choice of the hopping rate for unbound motor movements implies that the time scale τ is given by the diffusion coefficient D_{ub} of unbound motors via $\tau \equiv \ell^2/D_{\text{ub}}$. If it reaches a filament site, it binds to the filament with the sticking probability π_{ad} .

The behavior at the filament end has to be specified separately. We consider two possibilities: (i) active unbinding of motors at the filament end where motors at the last filament site make a forward step with rate α as at the other filament sites, but the latter step brings them to the forward non-filament neighbor site, so that their total unbinding probability is $\epsilon_0 + \alpha$, and (ii) thermal unbinding where a motor at the last filament site does not make a forward step, but has an increased waiting probability $\gamma' = \gamma + \alpha$. In that case, unbinding occurs with probability ϵ_0 .

The hopping rates can be chosen in such a way that one incorporates the measured transport properties of single motors such as velocity, diffusion coefficient, and average walking distance before unbinding from the filament [4,10].

Finally, motor-motor interactions can easily be incorporated into these models. In the following we mainly consider the mutual exclusion of motors from lattice sites. Exclusion is most important at filament sites (since the motors are strongly attracted to these sites), but in principle also applies to unbound motors. In the last section of this article, we consider cooperative binding of motors to the filament. In that case, the binding and unbinding probabilities depend on the occupation of the nearest neighbor filament sites.

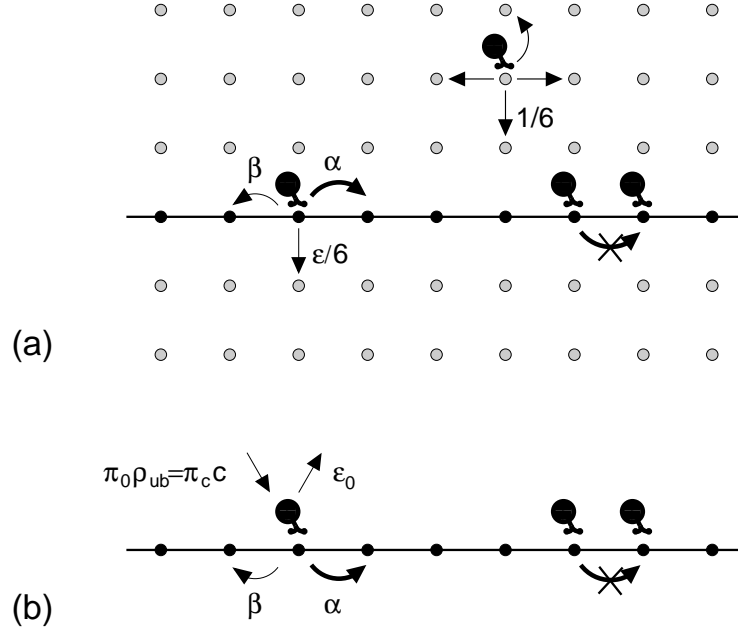


Fig. 1. Lattice model for molecular motor traffic: (a) Molecular motors step in a biased fashion along a filament (black line). With probability $\epsilon/6$, a motor unbinds from the filament by stepping to an adjacent non-filament site. Unbound motors perform symmetric random walks and, when reaching a filament site, rebind to it with probability π_{ad} . Mutual exclusion implies that motors cannot step to lattice sites that are already occupied by another motor. (b) In some situations, the unbound motor density ρ_{ub} (or the corresponding concentration c) can be considered as constant. In that case, bound motors move along the filament as in (a) and unbind from it with probability $\epsilon_0 = n_{ad}\epsilon/6$. Binding of a motor to an empty filament site occurs with probability $\pi_0 \rho_{ub} = n_{ad}\pi_{ad}\rho_{ub}/6$ which can also be expressed as $\pi_c c$ as discussed in section 4.

When considering many-motor systems, one is often interested in the motor densities and currents profiles rather than the single-motor trajectories. The quantities of main interest are then the bound and unbound motor densities ρ_b and ρ_{ub} . If gradients of the unbound motor density along the direction parallel to a filament can be neglected – either because unbound diffusion is very fast or because the space available for unbound diffusion is large, so that motors remain unbound for a long time before rebinding to the filament – the unbound density can be treated as constant. In that case, one obtains a one-dimensional model for the filament which is coupled to a reservoir of unbound motors with constant motor density as studied in Refs. [12,13,7,15,17]. Per unit time τ , a motor on the filament unbinds with probability ϵ_0 and binding of a motor from the reservoir to an empty lattice site occurs with probability $\pi_0 \rho_{ub} \equiv n_{ad}\pi_{ad}\rho_{ub}/6$, as shown in Fig. 1(b). This situation will be discussed in section 4.

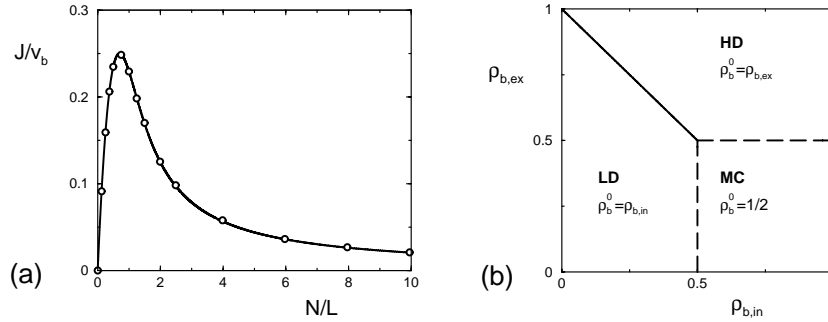


Fig. 2. (a) Bound motor current J for a filament in a tube with periodic boundary conditions as a function of the number N/L of motor particles per length within the tube. (b) Phase diagram for an open tube coupled to motor reservoirs with densities $\rho_{b,in}$ and $\rho_{b,ex}$ at the left and right end of the tube.

3 Motor traffic in tube-like compartments

The motor traffic through tube-like compartments in which one or several filaments are aligned parallel to the cylinder axis represents a simple system which mimics the transport in axons. We have studied tube-like systems with various kinds of boundary condition: closed systems [4,9,11], periodic boundary conditions [6], open boundaries coupled to motor reservoirs [6], and half-open systems [11].

The simplest case is given by periodic boundary conditions which can be solved exactly [6]. In this case, the stationary probability distribution is given by a product measure; the bound and unbound motor densities are constant and satisfy the radial equilibrium condition

$$\pi_{ad}\rho_{ub}(1 - \rho_b) = \epsilon\rho_b(1 - \rho_{ub}) \approx \epsilon\rho_b, \quad (1)$$

where the last approximation usually holds under experimentally accessible conditions, where the unbound density is small, but the bound motor density can be of the order of one motor per binding site. The bound motor current is given by $J = v_b\rho_b(1 - \rho_b)$ with the bound motor velocity v_b . As a function of the bound motor density or of the total number N of motors within the tube, it exhibits a maximum and decreases for high motor densities due to motor jamming as shown in Fig. 2(a).

If the tube is coupled to motor reservoirs at its orifices, the motor traffic exhibits boundary-induced phase transitions related to those of the one-dimensional asymmetric simple exclusion process (ASEP) [6]. As for the ASEP, a low-density, high-density and maximal-current phase are present, and correspond to situations where the bottleneck which limits the transport is given by the left boundary, the right boundary or the interior of the tube, respectively. In all three phases, the motor densities are approximately constant and satisfy radial equilibrium sufficiently far from the boundaries. The location of the transition lines within the phase diagram is quite sensitive to the precise choice of

the boundary conditions and can be shifted by tuning the model parameters. A particularly simple case is obtained if we impose radial equilibrium at the boundaries. In this case, the phase diagram, which is shown in Fig. 2(b), is independent of the motor transport properties and the geometric parameters of the tube, and the phase diagram corresponds exactly to the ASEP phase diagram.

4 Traffic jams on filaments in contact with a large motor reservoir

From an experimental point of view, the simplest system, for which one can study molecular motor traffic, is given by one or several immobilized filaments which are in contact with a solution with a certain motor concentration. For typical in vitro systems, unbound motor diffusion is very fast and the space available for unbound diffusion is large, so that we can describe the unbound motors by a constant density ρ_{ub} . In the following, we will use dimensionful quantities with units typically used by the experimentalist, and therefore characterize the unbound motors by the concentration c , which is typically in the nano-molar range, rather than by the local volume fraction ρ_{ub} . In these units, the rate for the binding of an unbound motor to an empty filament site is given by $\pi_c c$ where π_c is the second-order binding rate. It is related to the binding rate in density units via $\pi_c c = \pi_0 \rho_{\text{ub}}$ with $\pi_0 \equiv n_{\text{ad}} \pi_{\text{ad}}/6$ and is most conveniently expressed in terms of the dissociation constant $K_d \equiv \epsilon_0/\pi_c$ which has the dimension of concentration and is typically of the order of ~ 100 nM.

If the filament is long compared to the motor walking distance, the bound motor density is constant except for the regions close to the filament end and given by the equilibrium of the binding/unbinding dynamics, $\rho_{\text{b}}^{(0)} = c/(K_d + c)$ as shown in Fig. 3(a) and (b) for thermal and active unbinding at the filament end, respectively, using parameters for conventional kinesin. Likewise, the current along this part of the filament is given by $J_0 = v_{\text{b}} \rho_{\text{b}}^{(0)} (1 - \rho_{\text{b}}^{(0)})$. If the motors unbind thermally at the filament end, a (rather short) traffic jam forms at the filament end, where the motors accumulate. Note that no jam is obtained if the motors unbind actively as shown in Fig. 3(b).

The length of the jam region can be defined as $L_* \equiv L - x_*$ with the filament length L and $\rho(x_*) = (1 + \rho_{\text{b}}^{(0)})/2$. An estimate of L_* can be obtained from the balance of currents

$$J_0 - J_{\text{end}} = \epsilon_0 \int_{L-L_*}^L dx \left[\rho_{\text{b}} - \frac{c}{K_d} (1 - \rho_{\text{b}}) \right], \quad (2)$$

where J_{end} is the forward current at the last filament site. Eq. (2) leads to the jam length

$$L_* = \Delta x_{\text{b}} \frac{J_0 - J_{\text{end}}}{v_{\text{b}}} \left[\bar{\rho}_{\text{b,jam}} - \frac{c}{K_d} (1 - \bar{\rho}_{\text{b,jam}}) \right]^{-1}, \quad (3)$$

where $\bar{\rho}_{\text{b,jam}}$ is the average bound density in the jam region and Δx_{b} is the walking distance of the motors as given by $\Delta x_{\text{b}} \equiv v_{\text{b}}/\epsilon_0$.

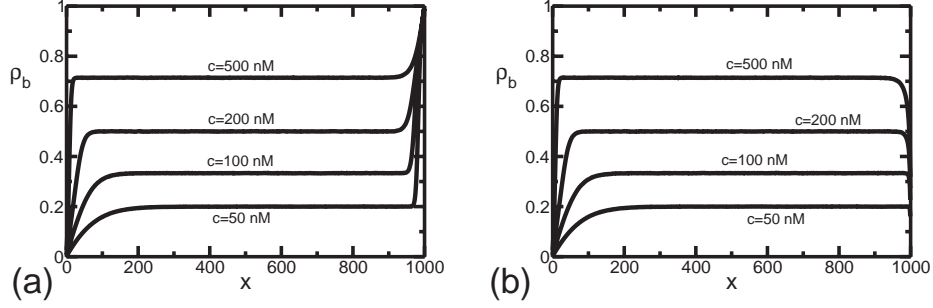


Fig. 3. Profiles of the bound motor density ρ_b on a filament in contact with a solution with constant unbound motor concentration c as a function of the coordinate x parallel to the filament for (a) thermal and (b) active unbinding at the filament end. Note that a traffic jam only occurs for thermal unbinding at the filament end and that this jam is rather short, of the order of the walking distance. The parameters are as appropriate for kinesin, $\epsilon_0 = 1/s$, $K_d = 200\text{nM}$, $v_b = 1\mu\text{m/s}$, and for a microtubule of length $8\mu\text{m}$.

For thermal unbinding of motors at the filament end, $J_{\text{end}} = 0$. If we estimate the density within the jam by the maximal value, $\bar{\rho}_{b,\text{jam}} \simeq 1$, Eq. (3) leads to

$$L_* \simeq \Delta x_b \frac{J_0}{v_b} \leq \Delta x_b / 4 \quad (4)$$

for the jam length in agreement with simulations which show that $L_* \simeq \Delta x_b J / v_b$ with a prefactor close to one.

This estimate shows that, for filaments in contact with a solution with constant motor concentration, the jam length L_* is of the order of the walking distance Δx_b . Longer jam lengths can arise (i) if the unbinding rate ϵ decreases with increasing density or (ii) if a gradient in the concentration of unbound motors is build up [4,9] which increases binding to the filament in the jam region and thus also increases the last term of Eq. (3).

5 Geometry-enhanced traffic jams in closed compartments

If filaments are embedded into closed compartments, the motor current along these filaments leads to the build-up of density gradients within these compartments [4,9,11]. These gradients are particularly pronounced in tube-like compartments where all filaments are aligned in parallel and with the same orientation along the tube axis. For low motor densities, the motors are essentially localized at that end of the tube towards which their active movements are directed. If exclusion can be neglected, the bound and unbound motor densities decrease exponentially if one moves away from this tube end. The length scale ξ of the exponential decrease is given by $\xi = D_{\text{ub}} \phi \epsilon / (v_b \pi_{\text{ad}})$, the ratio of the walking distance of bound motors and the distance unbound motor diffuse before rebinding.

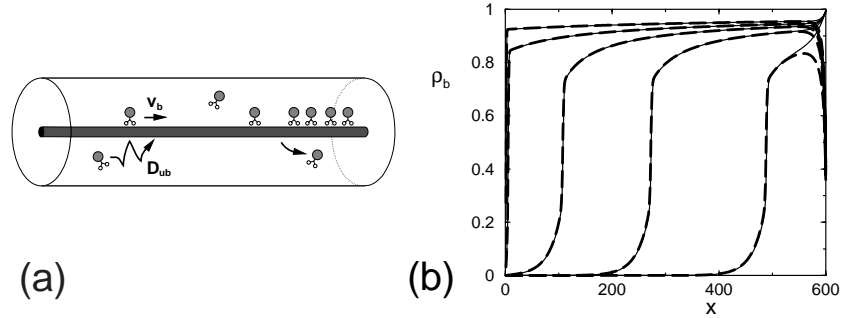


Fig. 4. (a) Motor traffic within a closed tube. The current of bound motors which move along a filament with velocity v_b is balanced by a diffusive current of unbound motors which diffuse back with the diffusion coefficient D_{ub} . (b) Corresponding profiles of the bound motor density ρ_b as a function of the coordinate x along the filament. A traffic jam domain at the right end of the tube builds up both for thermal and active unbinding of motors from the 'last' filament site (solid and dashed lines, respectively). With increasing overall motor concentration, the crowded domain spreads to the left.

In this expression, v_b and D_{ub} are the bound velocity and the unbound diffusion coefficient of the motors, respectively, and ϕ is the cross-section of the tube. A constant unbound motor density is a good approximation if $\xi \gg L$, i.e., for large unbound diffusion coefficients D_{ub} and for large tube radii.

If the overall motor density is increased in these systems, the region in which the motors are localized develops into an extended crowded domain, see Fig. 4. The length L_* of this domain defines the jam length for these systems. In contrast to the systems discussed in the previous section, the jam length can be larger than the walking distance and increases with increasing overall motor concentration until the crowded domain spreads over the full tube length. In this crowded domain, the density profiles can approximately be described by local radial equilibrium. For the case of a half-open tube, which is very similar to the closed tube, but more easily accessible to analytical methods, the latter approximation shows that the jam length scales essentially as $L_* \sim 1/v_b$ [11] rather than $L_* \sim \Delta x_b \sim v_b$ as for a filament in contact with a constant unbound motor density. The jam length is given by

$$L_* = \frac{\phi D_{ub} \pi_{ad}}{v_b \epsilon} G(\epsilon/\pi_{ad}, \rho_{b,in}), \quad (5)$$

where G is a function of the ratio of the binding and unbinding probabilities and of the bound motor density $\rho_{b,in}$ in the reservoir to which the tube is coupled at its open end [11]. If the boundary density is sufficiently close to one, G behaves as $G \approx -\ln(1 - \rho_{b,in})$ and the jam length diverges logarithmically with $1 - \rho_{b,in}$. For the closed tube, G is determined by an integral constraint which fixes the total number of motors within the tube.

In addition, the traffic jam is present for both thermal and active unbinding at the filament end [9] as shown in Fig. 4(b). This means that the crowded

domains are due to a combination of the motor behavior at the last filament site and the motor accumulation in the region close to the filament end. The latter accumulation is strongly geometry-dependent.

We have also studied centered or aster-like filament systems [9]. In this case, the accumulation of motors in the center of an aster is much weaker than in tube-like systems and, in fact, determined by a power law rather than by an exponential. As for filaments in contact with a reservoir with constant unbound motor density, traffic jams are obtained only for thermal unbinding at the filament end, but not for active unbinding. In addition, when the overall motor density is increased, the traffic jams remain short in this case. The main effect of an increase in the overall motor density is a flattening of the density profile.

6 Symmetry breaking and traffic lanes in systems with two motor species

Each molecular motor moves either towards the plus- or towards the minus-end of the corresponding filament, but different types of motors move into opposite directions along the same filament. In this situation, cooperative binding of the motors to the filament – in such a fashion that a motor is more likely to bind and less likely to unbind next to a bound motor moving in the same direction, while it is less likely to bind and more likely to unbind next to a motor with opposite directionality – leads to spontaneous symmetry breaking [7]: If the motor–motor interactions, which we characterize by a single interaction parameter q , are stronger than a certain critical interaction strength q_c , one motor species occupies the filament, while the other one is largely excluded from it. This symmetry breaking has been found both for tube-like compartments with periodic boundary conditions and for systems with a constant unbound motor density. In the latter case, symmetry breaking occurs, independent of the choice of the boundary conditions provided that the system size or the filament length is large compared to the motors' walking distance. Note that, in contrast to the previously reported example for symmetry breaking in a driven diffusive system, the 'bridge model' [31], the symmetry breaking here is not boundary-induced.

Symmetry breaking has two interesting consequences. First, it implies that for $q > q_c$ there is a discontinuous phase transition if the relative concentrations of the two motor species are varied. This transition is accompanied by hysteresis, which is again not boundary-induced, in contrast to the hysteresis which was reported recently for another driven diffusive system [32]. Second, if several filaments are aligned in parallel and with the same orientation, this symmetry breaking leads to the spontaneous formation of traffic lanes for motor traffic with opposite directionality [7].

7 Concluding remarks

The traffic phenomena in systems with many molecular motors can be described by stochastic lattice gas models which are similar to asymmetric exclusion pro-

cesses, but have the additional property that the motors can unbind from the filamentous track and diffuse in the surrounding fluid. These systems exhibit a variety of cooperative phenomena and, in addition to their importance for our understanding of the traffic within cells and for prospective applications in nanotechnology, provide promising model systems for the experimental study of driven diffusive systems.

References

1. J. Howard: *Mechanics of Motor Proteins and the Cytoskeleton* (Sinauer Associates, Sunderland 2001)
2. M. Schliwa, editor: *Molecular motors* (Wiley-VCH, Weinheim 2003)
3. M. Schliwa, G. Woehlke: *Nature* **422**, 759 (2003)
4. R. Lipowsky, S. Klumpp, T. M. Nieuwenhuizen: *Phys. Rev. Lett.* **87**, 108101 (2001)
5. T. M. Nieuwenhuizen, S. Klumpp, R. Lipowsky: *Europhys. Lett.* **58**, 468 (2002)
6. S. Klumpp, R. Lipowsky: *J. Stat. Phys.* **113**, 233 (2003)
7. S. Klumpp, R. Lipowsky: *Europhys. Lett.* **66**, 90 (2004)
8. T. M. Nieuwenhuizen, S. Klumpp, R. Lipowsky: *Phys. Rev. E* **69**, 061911 (2004)
9. S. Klumpp, T. M. Nieuwenhuizen, R. Lipowsky: *Biophys. J.* **88**, 3118 (2005)
10. R. Lipowsky, S. Klumpp: *Physica A* **352**, 53 (2005)
11. M. J. I. Müller, S. Klumpp, R. Lipowsky: *J. Phys.: Condens. Matter* **17**, S3839 (2005)
12. A. Parmeggiani, T. Franosch, E. Frey: *Phys. Rev. Lett.* **90**, 086601 (2003)
13. M. R. Evans, R. Juhász, L. Santen: *Phys. Rev. E* **68**, 026117 (2003)
14. V. Popkov, A. Rákos, R. D. Willmann, A. B. Kolomeisky, G. M. Schütz: *Phys. Rev. E* **67**, 066117 (2003)
15. G. Klein, K. Kruse, G. Cuniberti, F. Jülicher: *Phys. Rev. Lett.* **94**, 108102 (2005)
16. C. M. Arizmendi, H. G. E. Hentschel, F. Family: *Physica A* **356**, 6 (2005)
17. K. Nishinari, Y. Okada, A. Schadschneider, D. Chowdhury: *Phys. Rev. Lett.* **95**, 118101 (2005)
18. S. Katz, J. L. Lebowitz, H. Spohn: *J. Stat. Phys.* **34**, 497 (1984)
19. J. Krug: *Phys. Rev. Lett.* **67**, 1882 (1991)
20. A. B. Kolomeisky, G. M. Schütz, E. B. Kolomeisky, J. P. Straley: *J. Phys. A: Math. Gen.* **31**, 6911 (1998)
21. Y. Kafri, E. Levine, D. Mukamel, G. M. Schütz, J. Török: *Phys. Rev. Lett.* **89**, 035702 (2002)
22. K. Nagel, M. Schreckenberg: *J. Phys. I France* **2**, 2221 (1992)
23. D. Chowdhury, L. Santen, A. Schadschneider: *Phys. Rep.* **329**, 199 (2000)
24. S. Klumpp, R. Lipowsky: *Proc. Natl. Acad. Sci. USA* **102**, 17284 (2005)
25. I. Derényi, T. Vicsek: *Phys. Rev. Lett.* **75**, 374 (1995)
26. I. Derényi, A. Ajdari: *Phys. Rev. E* **54**, R5 (1996)
27. Y. Aghababaei, G. I. Menon, M. Plischke: *Phys. Rev. E* **59**, 2578 (1999)
28. S. Konzack: Funktion des Kinesin Motorproteins KipA bei der Organisation des Mikrotubuli-Cytoskeletts und beim polaren Wachstum von *Aspergillus nidulans*. Ph.D. thesis, Universität Marburg (2004)
29. S. Konzack, P. E. Rischitor, C. Enke, R. Fischer: *Mol. Biol. Cell* **16**, 497 (2005)
30. C. Leduc, O. Campàs et al.: *Proc. Natl. Acad. Sci. USA* **101**, 17096 (2004)
31. M. R. Evans, D. P. Foster, C. Godrèche, D. Mukamel: *Phys. Rev. Lett.* **74**, 208 (1995)
32. A. Rákos, M. Paessens, G. M. Schütz: *Phys. Rev. Lett.* **91**, 238302 (2003)